JPSE (Journal of Physical Science and Engineering), Vol. 8, No. 1, 2023, Page 20–35.
DOI: 10.17977/um024v8i12023p020

JPSE
(Journal of Physical Science and Engineering)

http://journal2.um.ac.id/index.php/jpse
EISSN: 2541-2485

Comparison of Microphysics Schemes on WRF-HAILCAST Model to Study Hailstone in Aeronautics (Case Study: Hail Strike on AirAsia A320-200, November 16, 2018)

Received
26 August 2022

Revised
30 November 2022

Accepted for Publication
16 January 2023

Published
04 July 2023

M I S Maulana* **and A Kristianto**

Department of Meteorology, School of Meteorology Climatology and Geophysics, Jl. Perhubungan I No. 5, South Tangerang, 15221, Indonesia.

***E-mail:** maulanaikko@gmail.com

Abstract
A hail strike is caused by the hail phenomenon, an aviation accident caused by environmental factors. Hail is a type of extreme weather in the form of precipitation ice grains which is generally caused by cumulonimbus clouds. Research on hail modeling can be carried out using the Weather Research Forecasting Hail Forecast (WRF-HAILCAST), which can model the structure, dynamics, microphysics, hailstone distribution, and estimate the maximum diameter of the hailstone. In this study, the hail modeling that caused the hail strike on the AirAsia A320-200 aircraft on November 16, 2018, was carried out using the WRF-HAILCAST model with six different microphysics schemes. This study compares the results of the microphysics scheme on the WRF-HAILCAST model in hail modeling. The results of this study indicated that each microphysics scheme produces a different outcome. Generally, the spatial and temporal distribution of the entire scheme could indicate the presence of convective clouds reaching 40–55 dBZ. Each scheme showed the microphysical processes of clouds consisting of different hydrometeor particles. However, only MY2 and NSSL showed the presence of supercooled water, and those schemes could estimate maximum diameter hailstone worth 25.8 mm and 13.2 mm. So, NSSL is the best microphysics scheme in this study.

Keywords: Hailstone, hail strike, WRF-HAILCAST, microphysics schemes.

1. Introduction

The airplane is transportation with high time efficiency and must be paid for with high costs and risk of accidents [1]. Based on flight accident data from 2016–2020 by the National Transportation Safety Commission (KNKT), there were 58 accidents and 123 severe incidents. Meanwhile, when reviewed from the leading causes of aviation accidents in 2016–2020, there were 51.38% caused by human factors, 14.08% caused by technical factors, 7.28% caused by environmental factors, and 2.28% caused by facility factors. One type of aviation accident caused by environmental factors is weather factors such as hail strikes. The effect of hail strikes in aviation is very significant if it hits the fuselage and may cause damage to the aircraft [2].

Hail is a type of extreme weather in the form of ice grains and a more than 5 mm diameter from cumulonimbus clouds [3]. The occurrence of hail in tropical latitudes is influenced by topographic factors and other patterns that play an essential role in hail occurrence at low latitudes [4]. The frequency of hail occurrences in tropical latitudes such as Indonesia is rare due to relatively warm surface air temperatures. However, deep convection associated with strong updrafts and downdrafts is common [5].

The instruments commonly used to detect hail are weather radar, weather satellites, and observations of surface and upper-air weather [6]–[8]. Those instruments have limitations that cannot represent the microphysical processes in the cloud and other processes that occur in the hail-producing cloud, so another approach is needed that can be used to analyze the results by using the

Weather Research Forecasting Hail Forecast (WRF-HAILCAST) model [9]. Research on hail simulation using WRF-HAILCAST in Indonesia still needs to be widely applied and needs further study. While research on simulation results using the WRF model has been widely carried out in Indonesia. WRF model with several microphysics parameterization schemes, which are WSM6, Thompson, Morrison-2, Goddard GCE, Milbrandt-Yau 2, and NSSL, can show good results in the simulation. The six schemes show cloud reflectivity values that reach more than 50 dBZ as the threshold, which indicates the presence of ice particles in the cloud that probably come down to the surface to produce hailfall. In addition, atmospheric dynamics conditions and microphysical processes in the cloud, such as strong vertical motion, high vertical relative humidity, and the estimated hailstone size, can be modeled reasonably well [5], [10]–[12].

This study used the WRF-HAILCAST model with several microphysics parameterizations to study the hailstone in the hail strike case on the AirAsia A320-200 with the DPS–JOG flight route and flight number AWQ8448 which allegedly occurred during cruising-descent on November 16, 2018 [13]. The impact of this hail strike caused damage to the cockpit and muzzle glass of the aircraft, and this case was chosen because hail strikes occur in Indonesian flights very rarely. This study focuses on the structure, microphysics, and dynamics of the hail-producing clouds in terms of weather radar and the outputs of the WRF-HAILCAST model.

2. Method

This study focused on the differences in using the microphysics scheme in the WRF-HAILCAST model to study the hailstone in the hail strike case on the AirAsia A320-200 flight on November 16, 2018, and to determine the best microphysics parameterization scheme in the hail modeling. The data used in this study is the initial model obtained from NCEP GDAS/FNL with a spatial resolution of 0.25° × 0.25° and a temporal resolution of 6 hours which is used as input data for hail modeling using WRF-HAILCAST. The data can be downloaded from https://rda.ucar.edu/ with the dataset code ds083.3. The data used is November 16, 2018, from 00.00–12.00 UTC, with the first 6 hours used as spin-up time. Another data used in this study is weather radar data obtained from BMKG. The time used is November 16, 2018, at 06.00–11.00 UTC, according to the time of the alleged hail strike based on the flight track log.

The tools used in this study were High-Performance Computing (HPC) from the National Research and Innovation Agency (BRIN), WRF Domain Wizard to determine the domain modeling (Figure 1), WRF version 4.0, GrADS, Rainbow 5, and Microsoft Excel. Model input data was processed using WRF-HAILCAST, while weather radar data was processed using Rainbow 5 software. After both data were successfully processed, analysis was carried out using the GrADS and Microsoft Excel software. The model configuration is shown in Table 1. This study set the cumulus parameterization scheme to no cumulus because the HAILCAST module can only be run in the no cumulus domain (4 km resolution or finer). Then the HAILCAST time step is set with a 0 (zero) code because HAILCAST is calculated every time the WRF run so that the HAILCAST time step follows the WRF time step, which is 50 seconds.

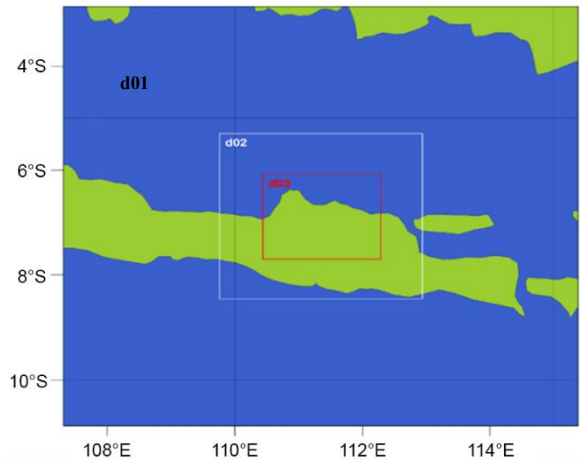

Figure 1. Domain configuration of WRF-HAILCAST.

Table 1. Model configuration of WRF-HAILCAST.

Configuration	Domain 1	Domain 2	Domain 3
Resolution grid	9 km	3 km	1 km
Temporal resolution	60 minutes	60 minutes	10 minutes
Time step	50	50	50
Spin up time	6 hours	6 hours	6 hours
e_we	100	118	205
e_sn	100	118	181
e_vert	35	35	35
HAILCAST time step	0	0	0
p_top_requested	50 hPa		
Center Latitude	6,879°S		
Center Longitude	111,349°E		
Microphysics	Morrison-2 (MORR)		
	WSM6 (WSM6)		
	Thompson Graupel (THOM)		
	Goddard GCE (GODD)		
	Milbrandt-Yau *2 moment* (MY2)		
	NSSL-*2 moment* (NSSL)		
Cumulus	No cumulus	No cumulus	No cumulus
Planetary Boundary Layer	YSU	YSU	YSU
Shortwave Radiation	Dudhia	Dudhia	Dudhia
Longwave Radiation	RRTM	RRTM	RRTM

3. Result and Discussion

3.1. Hail Strike Identification Using WRF-HAILCAST

Based on an initial analysis of the hail strike occurrence using data from https://avherald.com, weather radar observation data (Figure 2), and flight track log data (Table 2), the estimated hail strike time was between 09.32 and 09.40 UTC. During this time, the plane flew over Rembang, Pati, and Blora. At that location, weather radar data revealed the highest maximum reflectivity value of more than 50 dBZ. It indicates that the cloud has reached the cold cloud phase and its height has passed the freezing level, indicating that ice particles in the cloud could cause a hail strike on the aircraft. The coordinates location of the alleged hail strike based on the flight track log data are at -6.8595ºS and 111.1825ºE, whereas the maximum reflectivity value was in the interior cold (core) of the convective system cloud worth 50–55 dBZ at coordinates -6.896ºS and 111.093ºE was taken from the weather radar. However, there is a 2-minute difference in the estimated time of the incident based on the flight track log with radar observation data as a verifier. That is because the weather radar has a temporal resolution every 10 minutes, so the temporal resolution of the WRF-HAILCAST model is adjusted to the radar data.

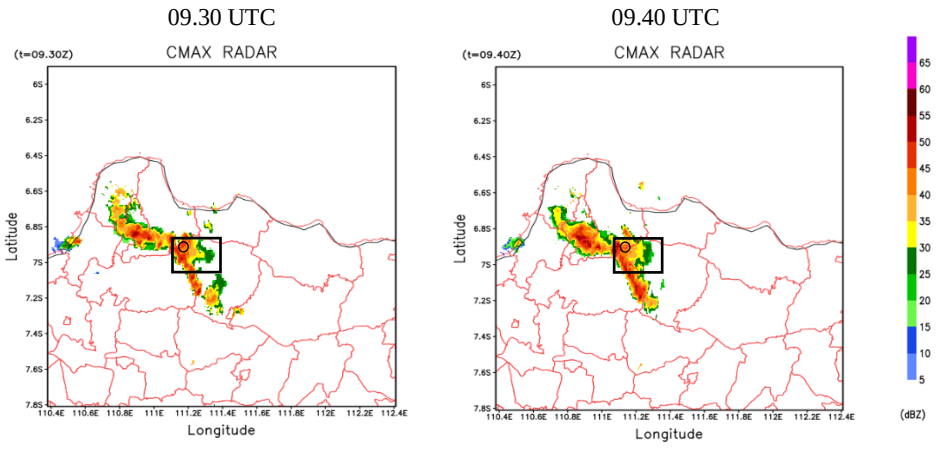

Figure 2. CMAX radar product. Black box showed the suspected location of hail strike, and the black circle showed the maximum reflectivity region.

Table 2. Flight track log AirAsia A320-200 on November 16, 2018.

Time	Latitude	Longitude	Course (°)	Speed (kt)	Speed (mph)	Altitude (m)	Explanation
03:56:53 PM	-8.7488	115.1245	270	186	214	465	Taking off
04:08:41 PM	-8.2621	114.0767	304	431	496	7018	Climbing
04:18:46 PM	-7.5641	113.0493	304	430	495	10478	Climbing
04:21:50 PM	-7.3561	112.7443	303	450	518	10973	Cruise
04:29:52 PM	-6.7336	112.0151	286	454	522	10965	Cruise
04:32:39 PM	-6.6472	111.6764	270	456	525	10927	Cruise
04:34:46 PM	-6.6462	111.4044	266	446	513	10020	Descending
04:35:38 PM	-6.6877	111.3135	229	414	476	9243	Descending
04:36:37 PM	-6.7702	111.2417	216	397	457	8931	Descending
04:37:32 PM	-6.8595	111.1825	217	406	467	8496	Descending
04:38:02 PM	-6.9019	111.1538	213	402	463	8176	Descending
04:39:24 PM	-7.0312	111.0678	215	381	438	7719	Descending
04:42:47 PM	-7.3296	110.8692	214	362	417	4869	Descending
05:17:59 PM	-7.7899	110.3865	88	150	173	351	Landing

Based on the maximum reflectivity values, it was discovered that between 09.30 UTC and 09.40 UTC, there was a convective system in the area where the hail strike was suspected (black box) with reflectivity values reaching 45–50 dBZ and maximum reflectivity values at the system's interior cold (core) cloud reaching 50–55 dBZ. The system moved to the northwest at 09.40 UTC, but the reflectivity value did not decrease. The WRF-HAILCAST model can also show the presence of a convective system in the alleged hail strike location region between 09.30 and 09.40 UTC. The location and pattern of the convective system, on the other hand, differed from that of CMAX weather radar products. Whereas the weather radar's maximum reflectivity was linear, the model's maximum reflectivity was circular.

The presence of two convective cloud cores around the suspected hail strike region is shown by MORR (Figure 3), WSM6 (Figure 4), THOMP (Figure 5), GODD (Figure 6), and NSSL (Figure 7), with the maximum reflectivity value in the convective cloud core being more significant than that indicated by weather radar, reaching 60–65 dBZ. At the same time, the MY2 microphysics scheme indicates the presence of one convective cloud core with a maximum reflectivity value of 55–60 dBZ in the area of the alleged hail strike. Only GODD and NSSL had the highest maximum reflectivity in the suspected area of 45-55 dBZ at 09.30 UTC, and NSSL decreased to 35–45 dBZ at 09.40, while GODD's reflectivity did not decrease. The scheme with the lowest maximum reflectivity value is THOMP at 20–40 dBZ at 09.30 UTC and 15–30 dBZ at 09.40 UTC.

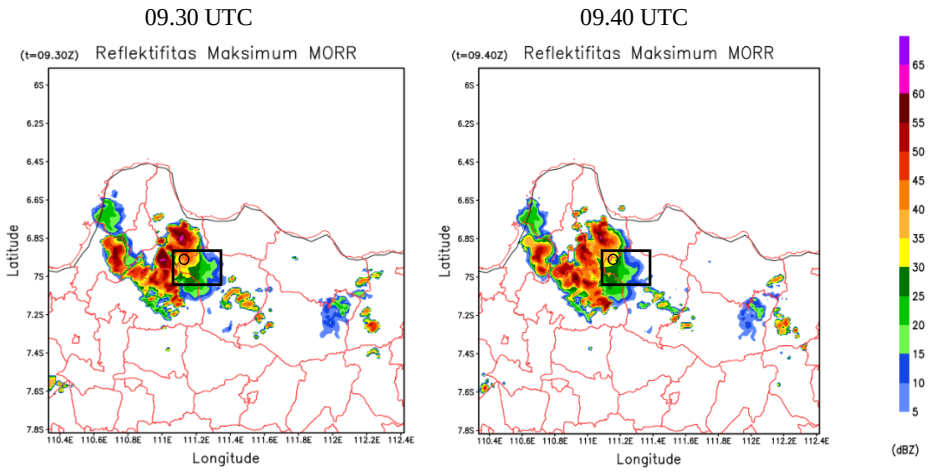

Figure 3. Maximum reflectivity of the model from MORR at 09.30 UTC and 09.40 UTC. Black box showed the suspected location of hail strike, and the black circle showed the maximum reflectivity region.

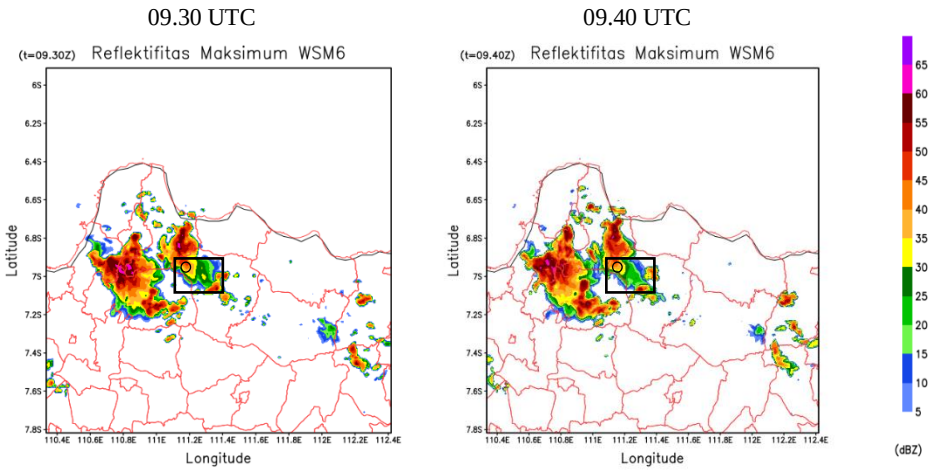

Figure 4. Maximum reflectivity of the model from WSM6 at 09.30 UTC and 09.40 UTC. Black box showed the suspected location of hail strike, and the black circle showed the maximum reflectivity region.

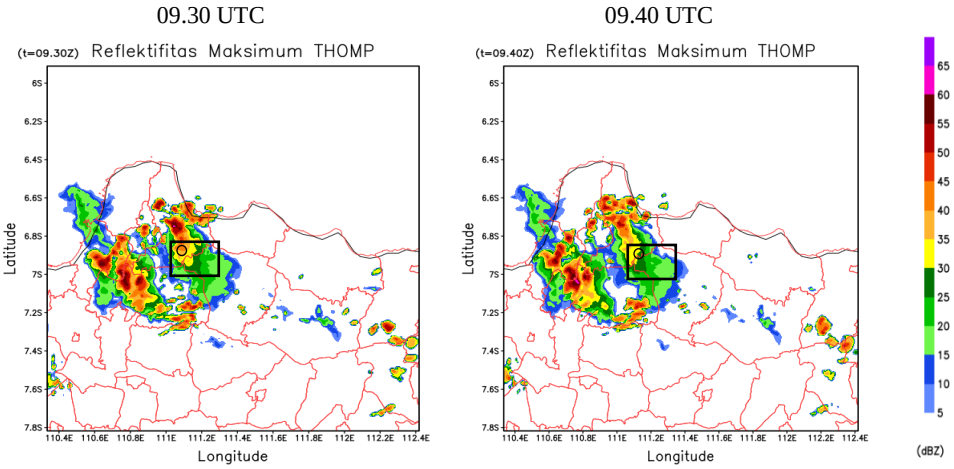

Figure 5. Maximum reflectivity of the model from THOMP at 09.30 UTC and 09.40 UTC. Black box showed the suspected location of hail strike, and the black circle showed the maximum reflectivity region.

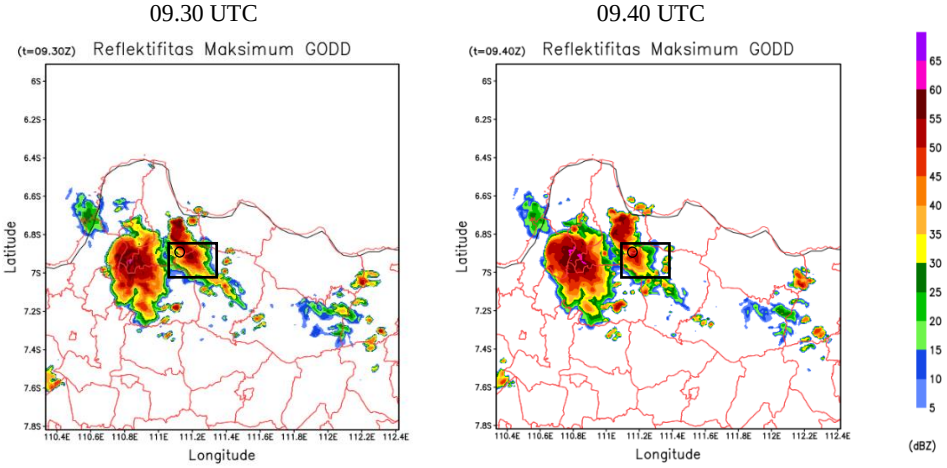

Figure 6. Maximum reflectivity of the model from GODD at 09.30 UTC and 09.40 UTC. Black box showed the suspected location of hail strike, and the black circle showed the maximum reflectivity region.

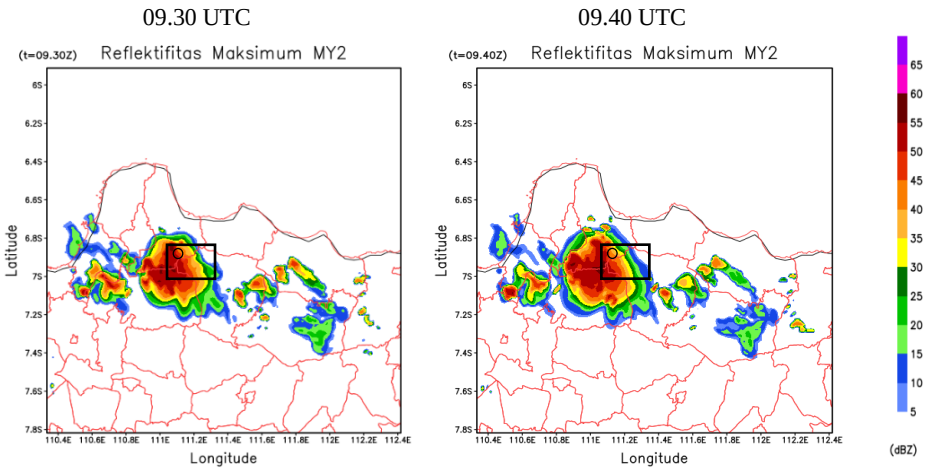

Figure 7. Maximum reflectivity of the model from MY2 at 09.30 UTC and 09.40 UTC. Black box showed the suspected location of hail strike, and the black circle showed the maximum reflectivity region.

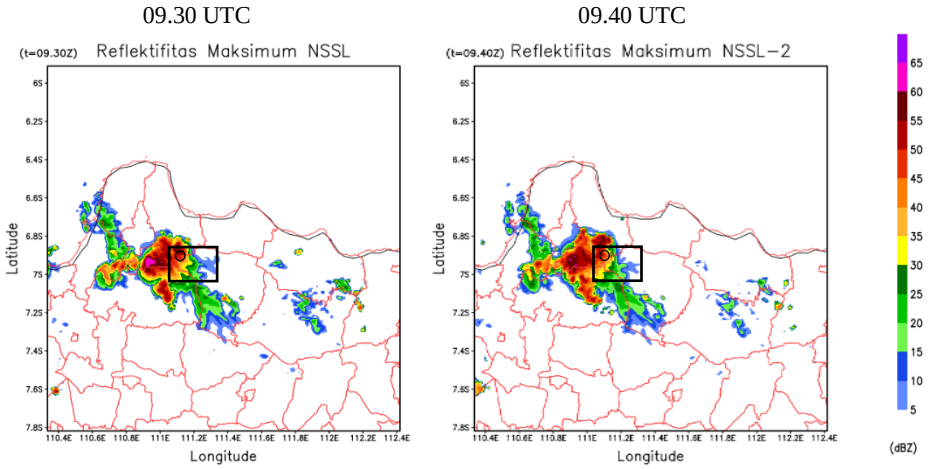

Figure 8. Maximum reflectivity of the model from NSSL at 09.30 UTC and 09.40 UTC. Black box showed the suspected location of hail strike, and the black circle showed the maximum reflectivity region.

3.2. Vertical Profile of Hail-Producing Cloud

The vertical reflectivity and vertical velocity parameters in Figures 9 and 10 depict the vertical profile of a hail-producing cloud. The location coordinates are adjusted to the weather radar coordinates, with the highest reflectivity values at -6.896ºS and 110.5º–111.25ºE. Vertical velocity can cause active cloud droplet areas at the top and bottom of convective clouds and influence cloud formation [14], [15]. The negative vertical velocity value indicates that air is moving downward (downdraft), and the positive vertical velocity value indicates that air is moving upward (updraft) [16].

At 09.30 UTC, the reflectivity value of convective clouds in the VCUT radar product (Figure 9) is 30–50 dBZ from layers 1–9 km. This reflectivity value indicates that the convective cloud has not yet matured enough to produce hail. At 09.40 UTC, a reflectivity pattern also ranged from 30–60 dBZ. Because small hailstone particles are concentrated above the freezing level layer and can be lifted to the top layer during an updraft, strong reflectivity patterns above the freezing level (i.e., 6–10 km or 450–270 mb) allow hail to occur. However, due to the lack of v component data in the radar at an elevation of 45º–90º, this radar image could not display the vertical velocity value. Thus, based on the image of this VCUT radar product, it can be seen that the most likely hail strike event occurred at 09.40 UTC.

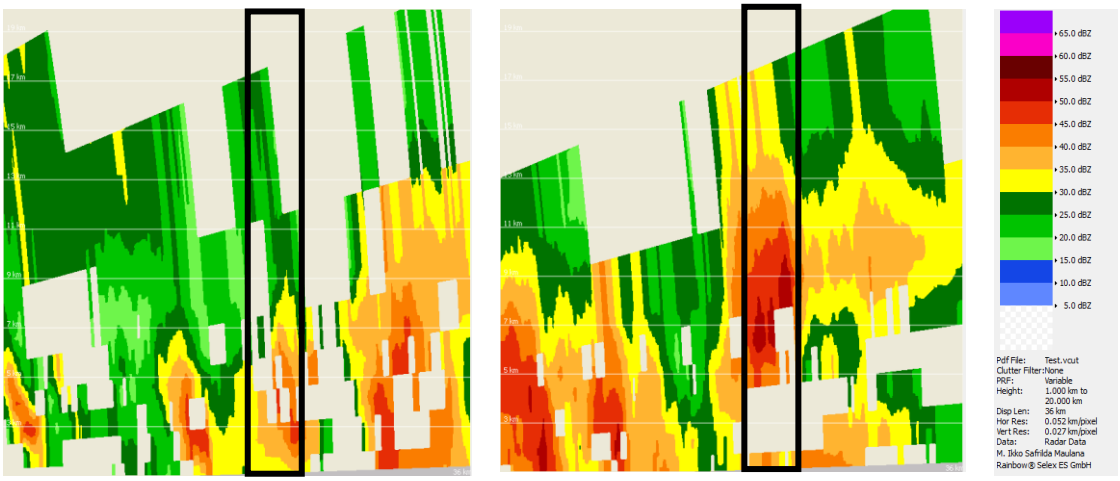

(a) (b)

Figure 9. VCUT radar product at (a) 09.30 UTC and (b) 09.40 UTC.

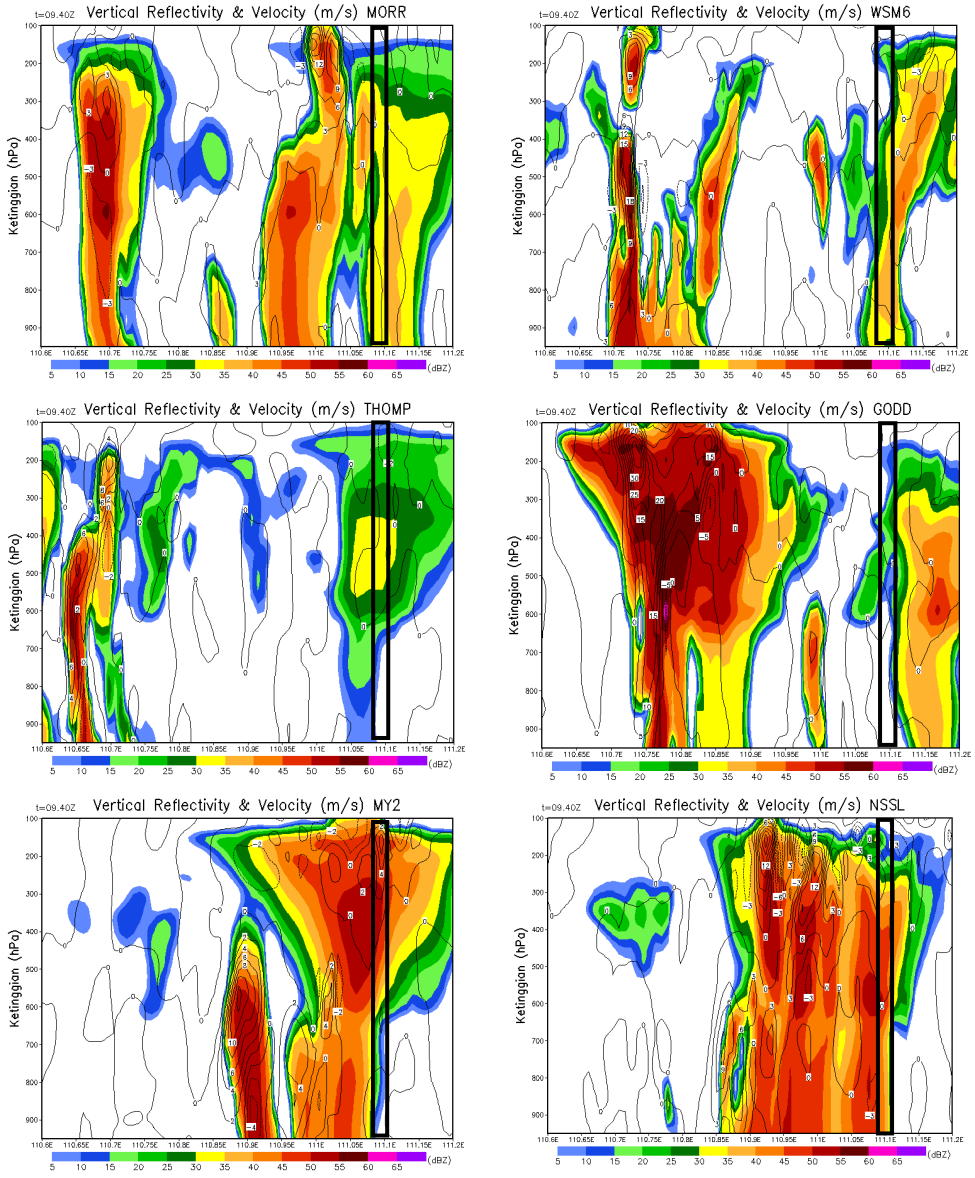

Figure 10. Vertical reflectivity and vertical velocity of the model at 09.40 UTC.

NSSL is the best scheme for simulating cloud reflectivity and vertical velocity, according to the output of the WRF-HAILCAST model (Figure 10). The cloud reflectivity value from the 950–250 mb layer is 45–60 dBZ. In the 900–800 mb layer, the vertical velocity parameter is -3 m/s. At the same time, in the 650–100 mb layer, the vertical velocity parameter is 0 m/s. This value indicates whether or not there is downward air movement (downdraft) in the lower layer. The increase in vertical velocity is accompanied by an increase in reflectivity to 55 dBZ, the majority of which is in the freezing level layer, indicating the presence of hailstone in the lower layer.

The vertical velocity parameter is the most difficult to estimate and has high uncertainty [17]. Updrafts, in particular, can be extremely valuable at times, but they are distributed randomly and quickly [18]. So, to demonstrate the presence of hailstone in the lower layers, it is necessary to examine the content of hydrometeor particles in the cloud and estimate the hailstone diameter.

Furthermore, an analysis of the skew-T diagram is carried out to estimate the height of the cloud tops, the altitude of the freezing level, the humidity of the air in each layer of the atmosphere, and the index of atmospheric lability. It is shown in Figure 11. The thick black line is the height of the cloud top, which is known by looking at the parcel temperature (purple line) and ambient temperature (red line). When the parcel's temperature exceeds the ambient temperature, it causes it to move up so that the top of the cloud becomes higher.

The highest cloud top height at 09.40 UTC was shown by MORR and MY2, which reached 13.5 km. At the same time, WSM6, THOMP, and NSSL reached 13 km. While GODD reached 12.5 km. Based on the height of the cloud tops and the freezing level, it can be seen that the cloud top height has passed the freezing level layer, so it will cause the water drops in the cloud to turn into drops that are too cold and graupel or ice. The presence of these particles can support ice formation in the cloud that occurs through the process of collision and coalescence between particles that are concentrated in the cloud [19].

The cloud top height followed the vertical cloud reflectivity analysis where MY2 and NSSL show higher reflectivity values in the upper layer so that the cloud top height of the scheme is higher than THOMP. Meanwhile, MORR, WSM6, and GODD developed a discrepancy between the vertical cloud reflectivity pattern and cloud top height from the skew-T diagram because the cloud top and vertical reflectivity data did not match. Although the WRF-HAILCAST model could describe the skew-T diagram well, the skew-T diagram from the results of this model could not be compared by observation because there was no sounding observation data around the incident area. So, this parameter is only used as an event estimator and does not describe the actual condition at the time of the incident.

When viewed from the freezing level height, which is determined by looking at the intersection point (orange line) between the ambient temperature (red line) and the isothermic line (blue line from bottom left to top right) at 0 ºC. From all schemes, at 09.40 UTC, generally at an altitude of 550 mb or about 4.9 km. That is under Indonesia's average freezing level, around 4.9 km [20], so the model can be used to properly determine the height of the freezing level.

At 09.40 UTC, the relative humidity in the 950–700 mb layer is 51–90%. At layer elevation above 700 mb, the schematic shows dry conditions (below 50%). The schematic shows the driest layer in the 500–150 mb layer. A dry atmosphere in the 700–500 mb layer may indicate an increase in the downdraft process and support convective clouds to produce hail. In addition, dry atmospheric conditions in the middle troposphere can lead to increased evaporative cooling in the near-surface layer and the formation of cold pools so that ice particles can retain their shape when falling at lower altitudes [21], [22].

In general, the atmospheric stability index shown by all schemes can represent an unstable atmosphere when the hail strike event is indicated by the Lifted Index (LI) value ranging from -3 K to -4 K in all schemes. Furthermore, the maximum Convective Available Potential Energy (CAPE) value is 1409 J/kg in the MY2 scheme, indicating moderate instability, thus supporting a hail strike.

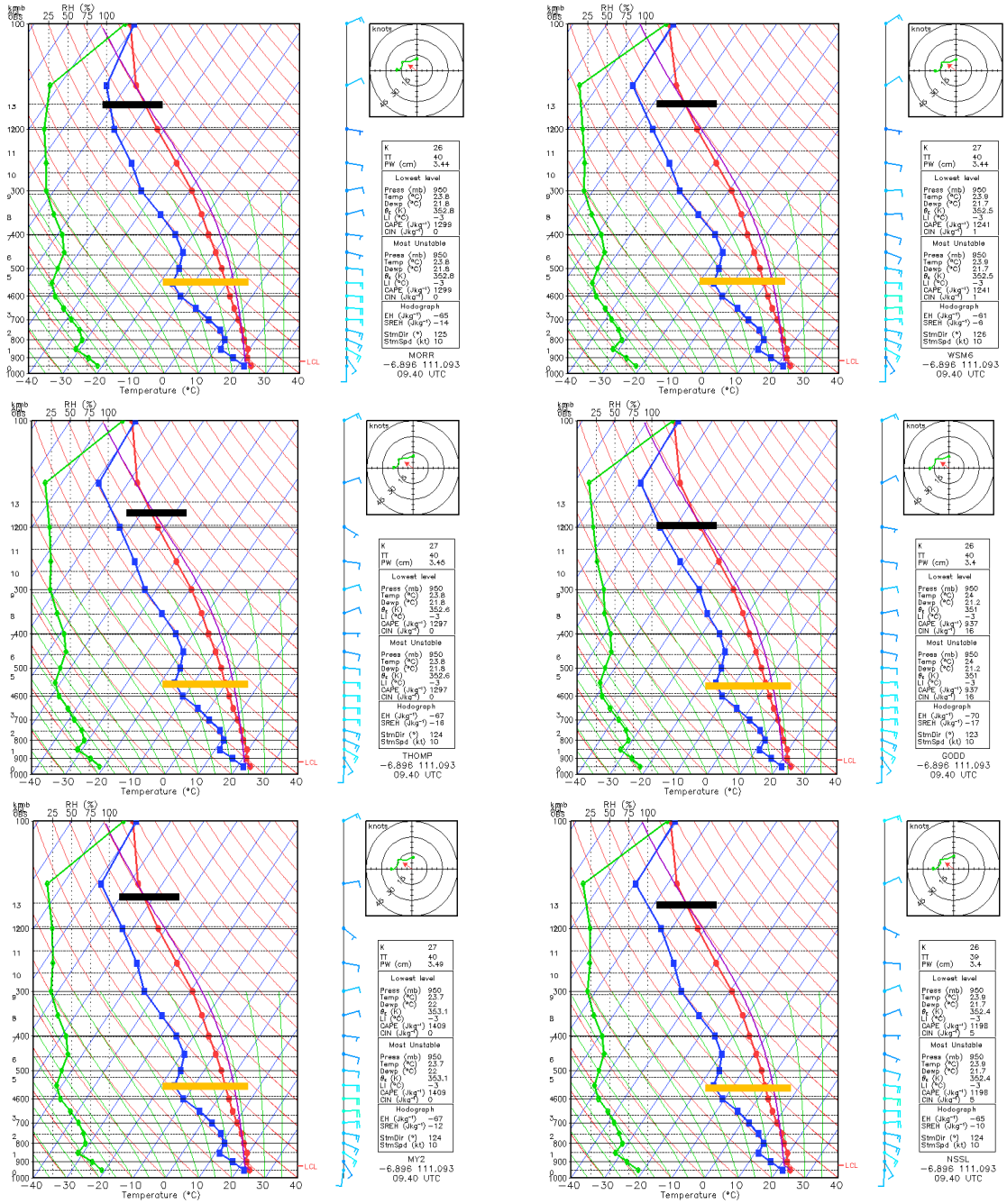

Figure 11. Skew-T diagram of the model at 09.40 UTC.

3.3. Cloud Microphysics During Hail Strike

Cloud microphysics analysis during the hail strike was carried out to determine the distribution of hydrometeor particles in the cloud. Figure 12 shows the accumulated mixing ratio of each type of cloud hydrometeor particle vertically from the output of the WRF-HAILCAST model at 09.30 UTC until 09.40 UTC.

All schemes generally show the same pattern in the distribution of water vapor particles in the atmosphere during the hail strike. Water vapor particles are present in the surface layer up to 100 mb or above the freezing level layer. The highest mixing ratio value reaches 26–34 g/kg at the height of 950 mb to 100 mb. The presence of water vapor particles above the freezing level layer can cause water vapor to be deposited into ice or produce hail embryos directly without passing through the liquid phase [23].

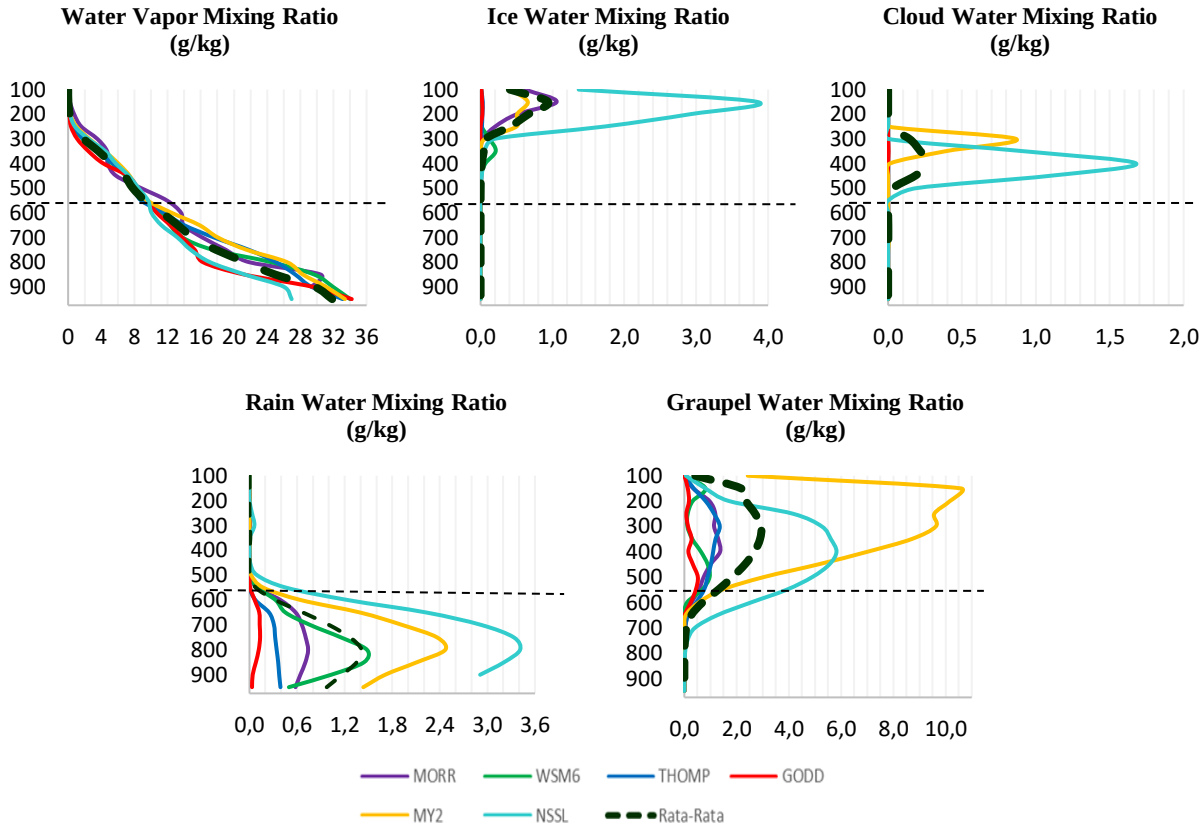

Figure 12. The accumulation of mixing ratio for each type of hydrometeor particle as a result of the WRF-HAILCAST model vertically at 09.30-09.40 UTC.

Then, the ice particles show the most negligible concentration during the hail strike. Ice particles' highest mixing ratio value reached 3.9 g/kg in the NSSL scheme. The entire schematic shows the presence of ice particles accumulating at the cloud top. The presence of ice particles above the freezing level layer makes a small contribution to the formation and development of hail particles in the cloud when a hail strike occurs [18].

Cloud water particles or cloud water can only be generated by the GODD, MY2, and NSSL schemes in the 09.30–09.40 UTC range. The highest mixing ratio value was shown by NSSL, which reached 1.68 g/kg, and GODD indicated the lowest mixing ratio value at 0.003 g/kg. The three schemes show cloud water particles above the freezing level layer, which interprets that the hydrometeor particles are already in the supercooled water phase or the drops are too cold. The presence of supercooled water in the cloud and upward airflow can contribute to the formation of graupel through an efficient merging process, where cloud water particles can grow and turn into rainwater. Furthermore, rainwater contributes to the formation of graupel [24].

Rainwater particles can be generated often when the hail strike occurs at 09.30–09.40 UTC. MY2 and NSSL produced the most rainwater particles in the 950 mb to 500 mb layers, with the highest values of 2.47 g/kg and 3.41 g/kg, respectively. From all schemes, only MORR and NSSL produce rainwater particles up to a layer of 300 mb or about 9 km, but the total concentration of NSSL is much higher than the MORR 0.062 g/kg in that layer. The presence of rainwater particles above the freezing level layer indicates that the rainwater is already in the supercooled water phase. The presence of supercooled water is also one of the things that play an essential role in the formation of hail because the ice particles and supercooled water will experience a collision and coalescence process due to the terminal velocity, which causes the supercooled water particles to freeze directly on top of the ice particles so that the particle diameter becomes more extensive due to concentrated supercooled water and ice particles [19], [25].

Furthermore, the highest number of graupel particle concentrations from all schemes is at an altitude above 13 km. The MY2 and NSSL schemes showed the highest concentrations compared to all other schemes, which reached 10.58 g/kg and 5.82 g/kg, respectively. The whole scheme can generally produce graupel particles below the freezing level layer. However, the amount of concentration is different in each scheme. NSSL shows the highest value of 2.56 g/kg below the freezing level layer. The presence of graupel particles under the freezing level layer indicates that the hail is small and allows it to fall to the surface because it can survive after passing the freezing level layer [5].

Of all the hydrometeor particles discussed, all schemes can show the presence of cumulonimbus clouds which contain various mixtures of water particles, supercooled water, graupel, or hail. However, only the NSSL scheme can show the best cloud microphysics and may cause a hail strike. That is because NSSL produces the highest amount of graupel concentration below the freezing level layer or near the surface, so it can be a strong indication to produce a hail strike.

3.4. Hailstone Distribution and Maximum Diameter Hailstone

Determination of the distribution and size of the maximum hailstone diameter from each microphysics scheme is best done by reviewing the results of ZHAIL product radar images with a certain threshold based on previous research [7]. The ZHAIL product is a radar product algorithm that detects three-dimensional reflectivity data. This product analyzes the vertical structure of the reflectivity above the freezing level by taking into account the height of the freezing level layer, the thickness of the hail layer above the freezing level, and the echo value at the highest altitude corrected by the effect of the radar beam [14], [15]. Figure 13 shows ZHAIL products at 09.30 and 09.40 UTC.

Based on the ZHAIL product radar image with a threshold of 45 dBZ (Figure 13), the hail has the potential to occur with a probability of more than 90% in the area where the hail strike is suspected at 09.40 UTC. Meanwhile, at 09.30 UTC, the maximum probability of a result is 40%. So, the hail time occurrence may occur at 09.40 UTC.

The WRF-HAILCAST model can produce estimates of the distribution and diameter of yield particles that have the potential to reach the surface based on calculations obtained from the updraft profile of each atmospheric layer in the cumulonimbus cloud shown in Figure 14 and Figure 15 of each microphysics scheme. The greater the updraft value generated by the model calculations in the cumulonimbus cloud, the greater the estimated diameter of the resulting hailstone will be [11].

Figure 14 shows the results of estimating the hailstone's maximum diameter that best matches the location of the alleged hail strike, namely MY2 and NSSL, with a maximum diameter of 25 mm and 14 mm at 09.30 UTC. In contrast, other schemes could not show the presence of hailstone at the alleged hail strike location.

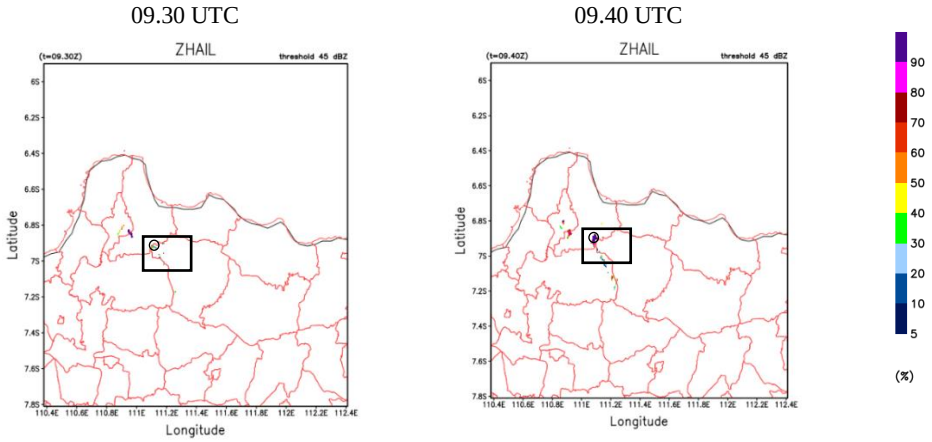

Figure 13. ZHAIL radar product with 45 dBZ threshold at 09.30 UTC and 09.40 UTC.

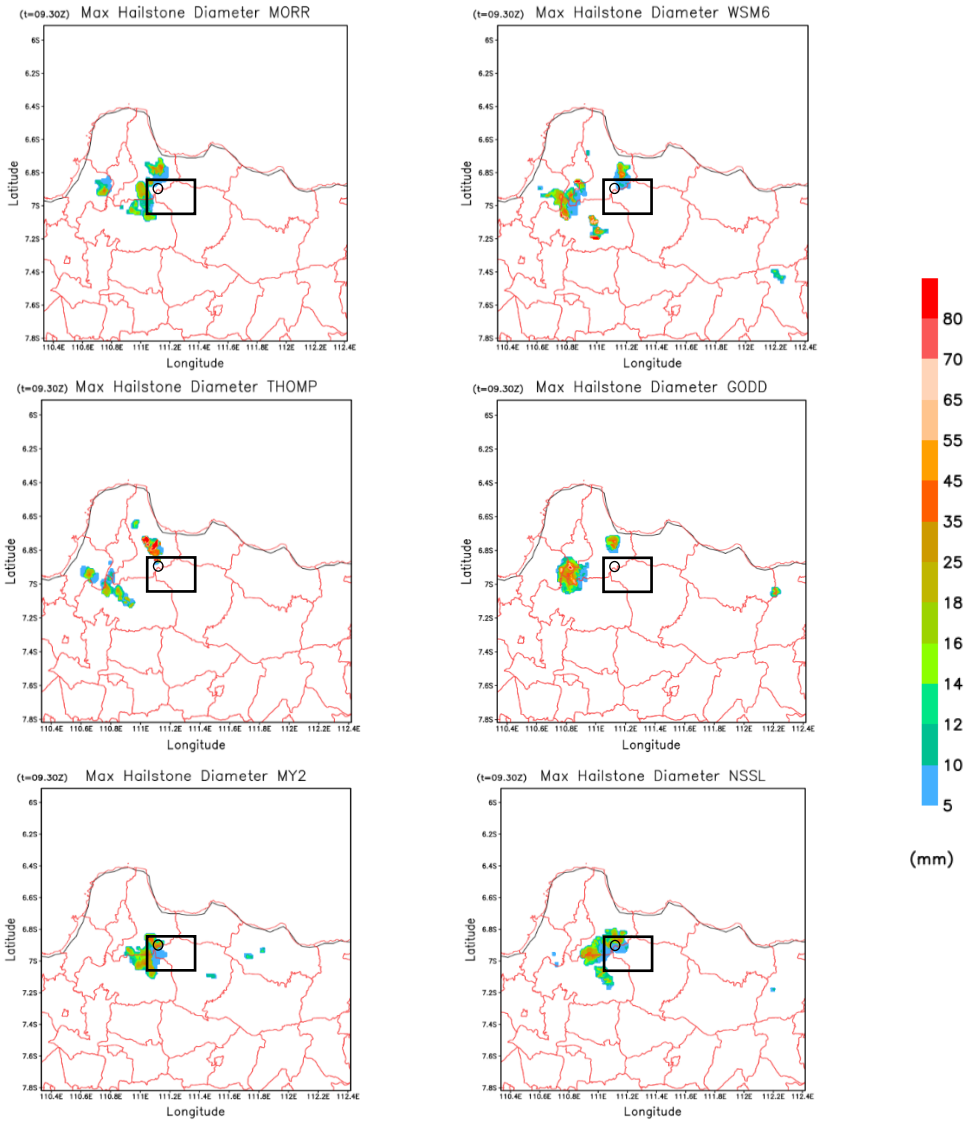

Figure 14. The distribution and size of the maximum hailstone diameter at 09.30 UTC on each scheme.

Furthermore, Figure 15 shows the results of estimating the maximum diameter of the hailstone that most closely matches the location of the alleged hail strike, namely the NSSL scheme, with the highest value reaching 10 mm at 09.40 UTC. Compared with the estimation result at 09.30 UTC, the maximum diameter of the hailstone at 09.40 UTC is smaller. In addition, other microphysical schemes cannot show the estimated maximum size of the hailstone diameter at the location of the alleged hail strike. However, from all schemes that show the largest estimated maximum size of the hailstone outside the alleged location of the hail strike, it is shown by THOMP and WSM6. So, the scheme tends to overestimate in estimating the maximum size of the hailstone diameter.

Each scheme shows different results when viewed from the distribution of the maximum size in other locations, with the highest estimated maximum hailstone size value of THOMP and WSM6, which reached 80 mm. The existence of areas of potential hail occurrence in other locations cannot be verified by observation because of the unavailability of hailstone observation, so it is not possible to know if the estimated distribution of hail in other locations may or may not occur.

Figure 16 shows the hailstone development by time at -6.896ºS and 111.093ºE according to the alleged hail strike location coordinates and the ZHAIL radar product. In general, each microphysical scheme produces a different estimate of the maximum size of the hailstone diameter. It is because each microphysical scheme considers particles resulting from different updraft values. The higher the updraft generated by the microphysical scheme, the greater the estimated maximum diameter size of the resulting hailstone.

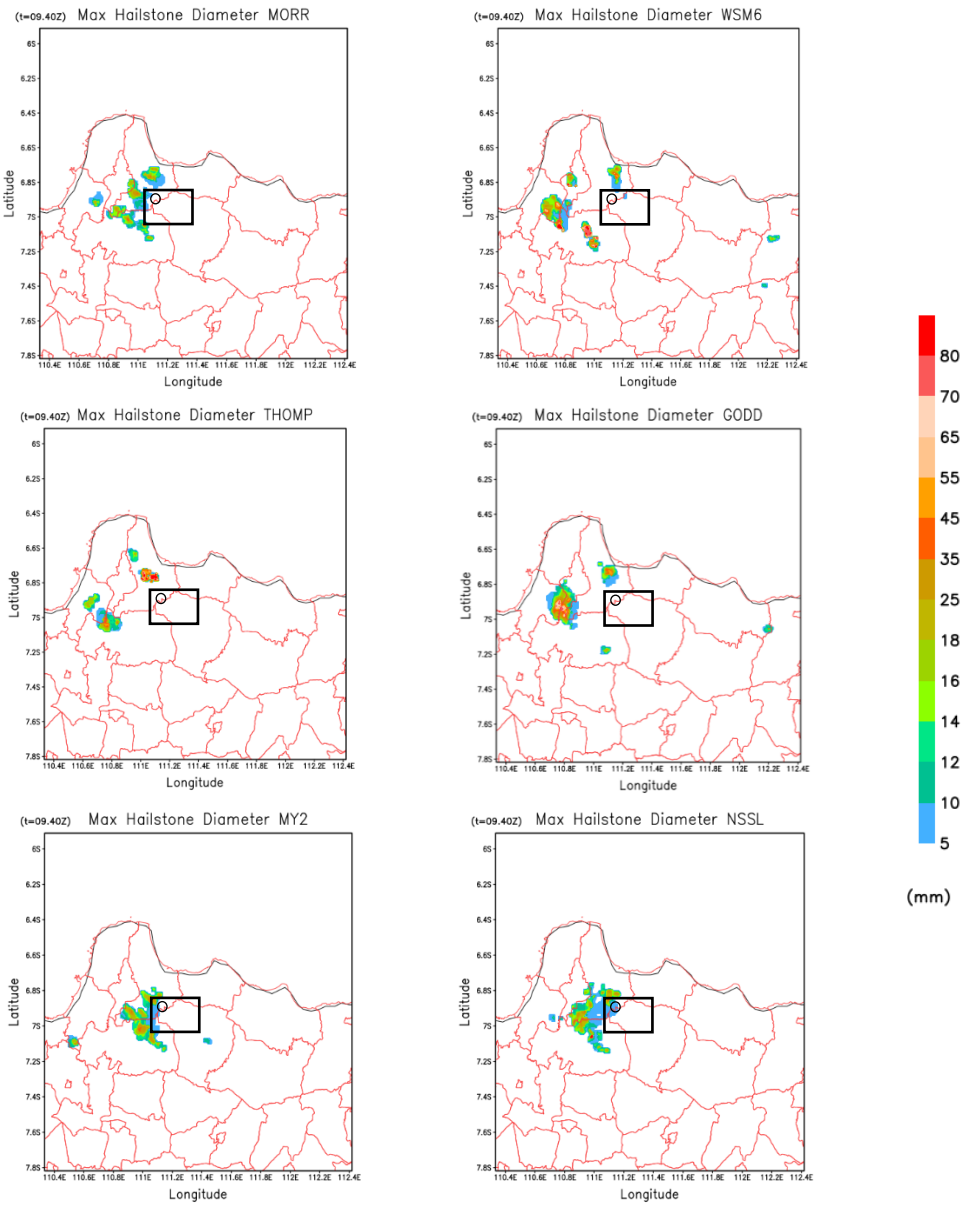

Figure 15. The distribution and size of the maximum hailstone diameter at 09.40 UTC on each scheme.

Figure 16 shows that the MORR results in the earliest hail event occurring at 08.10 UTC, with the maximum estimated value of hailstone diameter being 17.3 mm. Furthermore, results occur in the GODD, NSSL, MY2, WSM6, and THOMP schemes. However, the ones that can show the best results are MY2 and NSSL. The estimated maximum hailstone size generated by MY2 at 09.30 UTC is 25.8 mm and at 09.40 UTC is 9.1 mm. Meanwhile, NSSL produces an estimated maximum hailstone size of 9.7 mm at 09.30 UTC and 09.40 UTC. Observation data cannot verify this estimation result because the weather radar used cannot estimate the diameter of the hailstone particle at the time of the incident. After all, it uses a single polar Doppler weather radar whose specifications can only detect the direction and movement of particles in the atmosphere and observe the intensity of precipitation and object velocity.

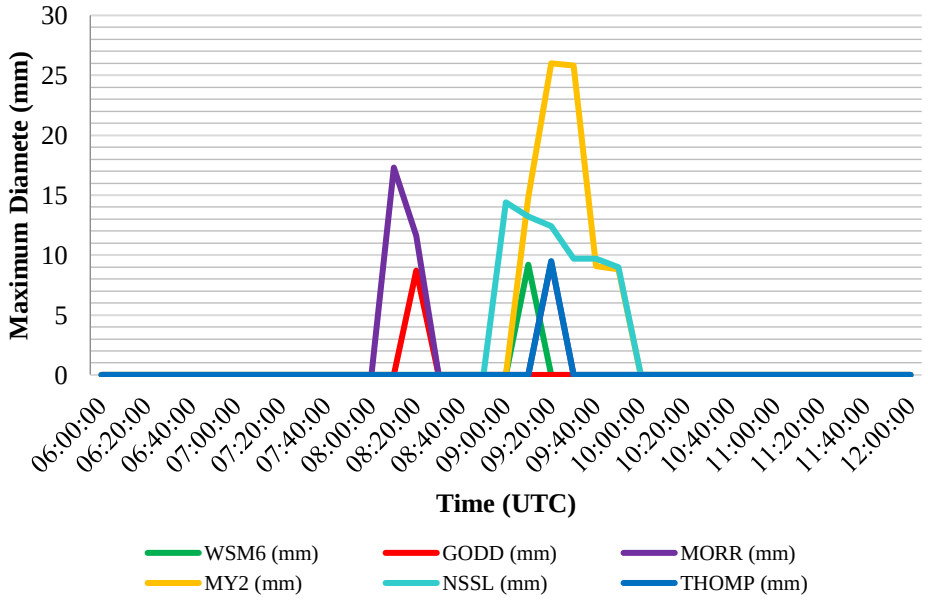

Figure 16. The graph of the development of the hailstone against time every 10 minutes of each microphysics scheme.

4. Conclusion

Based on the research that has been carried out, it can be concluded that each microphysics parameterization scheme can provide different outcomes in modeling the hail event in the case of the hail strike accident on the AirAsia A320-200 flight on November 16, 2018, spatially and temporally, the entire scheme can show the existence of convective clouds or cumulonimbus clouds with different patterns, extent, structure, and cloud microphysics when hail occurs. MORR, WSM6, GODD, MY2, and NSSL showed spatial reflectivity values reaching 45–55 dBZ except for THOMP, which only reached 40 dBZ at 09.30–09.40 UTC. The height of the cloud tops and the value of the atmospheric stability index indicate the presence of cumulonimbus clouds that grow to 12.5–13.5 km. Each schematic shows a cloud microphysics process consisting of rainwater, water vapor, graupel, and ice. However, only the MY2 and NSSL schemes show the presence of supercooled water particles. The presence of supercooled water particles dramatically affects the graupel formation process, so the concentration of graupel in MY2 and NSSL is the highest. The results of the spatial distribution of hailstone particles from MY2 and NSSL show the presence of hailstone around the location of the alleged hail strike and the estimated maximum size of the hailstone diameters are 25.8 mm and 13.2 mm, respectively. So, NSSL is a microphysics scheme that shows the best results in this modeling.

Acknowledgment

The authors would like to thank those who have assisted in preparing this article until it is appropriately completed, namely the National Research and Innovation Agency (BRIN), which has lent access to High-Performance Computing (HPC). Mr. Muchamat Agus Fitrianto, S.T., has assisted in the data request process.

References

[1] A. Kristianto, I. J. A. Saragih, G. Larasati, and K. Akib, "Identifikasi kejadian hujan es menggunakan citra radar dan satelit cuaca," *Pros. PIT Ke-5 Ris. Kebencanaan Univ. Andalas*, Padang, May 2–4, 2018, pp. 349–362.

[2] L. Yin, F. Ping, and J. Mao, "Impact of cloud microphysical processes on the simulation of a hailstorm in East China," *Atmos. Res.*, vol. 219, pp. 36–56, May 2019, doi: 10.1016/j.atmosres.2018.12.014.

[3] N. M. Sani and R. Gernowo, "Analisis turbulensi pada pesawat Etihad Airways EY-474 tanggal 4 Mei 2016 dengan metode weather research and forecasting," *Youngster Phys. J.*, vol. 7, no. 1, pp. 34–39, Jun. 2018.
[4] J. R. Holton, *An Introdution to Dynamic Meteorology*, 4th ed. Burlington, MA, USA: Elsevier Academic Press, 2004.
[5] M. D. Syaifullah, "Analisis kondisi udara atas wilayah Indonesia dengan data radiosonde" *J. Meteorol. Geofis.*, vol. 18, no. 1, Nov. 2017, pp. 1–12, doi: 10.31172/jmg.v18i1.268.
[6] J. Labriola, N. Snook, M. Xue, and K. W. Thomas, "Forecasting the 8 May 2017 severe hail storm in Denver, Colorado, at a convection-allowing resolution: Understanding rimed ice treatments in multimoment microphysics schemes and their effects on hail size forecasts," *Mon. Weather Rev.*, vol. 147, no. 8, pp. 3045–3068, Aug. 2019, doi: 10.1175/MWR-D-18-0319.1.
[7] D. McCann and M. Aviation, "Forecasting hail aloft," in *18th Conf. Aviat., Range, Aerosp. Meteorol.*, Seattle, Jan. 22–26, 2017, p. 212.
[8] F. P. Sari, A. P. Baskoro, and O. S. Hakim, "Effect of different microphysics scheme on WRF model: A simulation of hail event study case in Surabaya, Indonesia," in *AIP Conf. Proc.*, vol. 1987, no. 1, p. 020002, Jul. 2018, doi: 10.1063/1.5047287.
[9] R. D. Adams-Selin *et al.*, "Evolution of WRF-HAILCAST during the 2014–16 NOAA/hazardous weather testbed spring forecasting experiments," *Weather Forecast.*, vol. 34, no. 1, pp. 61–79, Feb. 2019, doi: 10.1175/WAF-D-18-0024.1.
[10] N. Ayasha, "Kajian analisis parameter vertical velocity dan kaitannya dengan kondisi parameter cuaca saat kejadian hujan es," *Bul. GAW Bariri*, vol. 3, no. 1, pp. 17–24, Aug. 2022, doi: 10.31172/bgb.v3i1.64.
[11] R. D. Adams-Selin and C. L. Ziegler, "Forecasting hail using a one-dimensional hail growth model within WRF," *Mon. Weather Rev.*, vol. 144, no. 12, pp. 4919–4939, Dec. 2016, doi: 10.1175/MWR-D-16-0027.1.
[12] J. M. Wallace and P. V. Hobbs, *Atmospheric Science: An Introductory Survey*, 2nd ed. Burlington, MA, USA: Elsevier Academic Press, 2006.
[13] K. E. Kunkel *et al.*, "Monitoring and understanding trends in extreme storms: State of knowledge," *Bull. Am. Meteorol. Soc.*, vol. 94, no. 4, pp. 499–514, Apr. 2013, doi: 10.1175/BAMS-D-11-00262.1.
[14] SELEX, *Software Manual Rainbow 5 Product & Algorithms*. Neuss, Germany: SELEX Sistemi Integrati GmbH, 2013.
[15] B. H. K. Tjasyono, *Klimatologi*, 2nd ed. Bandung, Indonesia: ITB Press, 2004.
[16] A. Khain, T. V. Prabha, N. Benmoshe, G. Pandithurai, and M. Ovchinnikov, "The mechanism of first raindrops formation in deep convective clouds," *J. Geophys. Res.: Atmos.*, vol. 118, no. 16, pp. 9123–9140, Jul. 2013, doi: 10.1002/jgrd.50641.
[17] D. Martínez-Castro *et al.*, "The impact of microphysics parameterization in the simulation of two convective rainfall events over the central Andes of Peru using WRF-ARW," *Atmos.*, vol. 10, no. 8, p. 442, Aug. 2019, doi: 10.3390/atmos10080442.
[18] Badan Meteorologi Klimatologi dan Geofisika. (2010, Oct. 7). *Peraturan Kepala Badan Meteorologi, Klimatologi, dan Geofisika Nomor: Kep. 009 Tahun 2010 Tentang Prosedur Standar Operasional Pelaksanaan Peringatan Dini, Pelaporan, dan Diseminasi Informasi Cuaca Ekstrim*. [Online]. Available: https://peraturan.bpk.go.id/Home/Details/191418/perka-bmkg-no-kep9-tahun-2010
[19] S. Zhang, S. Liu, and T. Zhang, "Analysis on the evolution and microphysical characteristics of two consecutive hailstorms in spring in Yunnan, China," *Atmos.*, vol. 12, no. 1, p. 63, Jan. 2021, doi: 10.3390/atmos12010063.
[20] B. H. K. Tjasyono, *Mikrofisika Awan dan Hujan*. Jakarta, Indonesia: Badan Meteorologi, Klimatologi, dan Geofisika, 2012.
[21] M. Frystine, A. Mulya, A. Kristianto, and M. P. Maulidyah, "Analysis of atmospheric condition on hail event at Pelalawan (Case study: September 23rd, 2019)," *J. Meteorol. Geofis.*, vol. 23, no. 2, pp. 45–56, Jun. 2022, doi: 10.31172/jmg.v23i3.813.
[22] Komite Nasional Kecelakaan Transportasi, "Laporan Statistik 2020." knkt.go.id. http://knkt.go.id/post/read/buletin-knktedisi-januari---maret-2020 (accessed Jan. 22, 2022).

[23] C. D. Ahrens and R. Henson, *Meteorology Today: An Introduction to Weather, Climate and the Environment*, 11th ed. Boston, MA, USA: Cengage Learning, 2015.
[24] M. Karalis *et al.*, "Effects of secondary ice processes on a stratocumulus to cumulus transition during a cold-air outbreak" *Atmos. Res.*, vol. 277, p. 106302, Oct. 2022, doi: 10.1016/j.atmosres.2022.106302.
[25] S. Hradecky, "Incident: Indonesia AirAsia A320-200 at Jogjakarta on Nov 16th 2018, hail strike." The Aviation Herald. http://avherald.com/h?article=4c07f42a&opt=0 (accessed Jan. 15, 2022).